

An optimized target-field method for MRI transverse biplanar gradient coil design

Rui Zhang¹, Jing Xu¹, Youyi Fu², Yangjing Li², Kefu Huang¹,
Jue Zhang^{1,2} and Jing Fang^{1,2}

¹ College of Engineering, Peking University, Beijing 100871, People's Republic of China

² Academy for Advanced Interdisciplinary Studies, Peking University, Beijing 100871, People's Republic of China

E-mail: zhangjue@pku.edu.cn

Received 18 September 2011, in final form 11 October 2011

Published 15 November 2011

Online at stacks.iop.org/MST/22/125505

Abstract

Gradient coils are essential components of magnetic resonance imaging (MRI) systems. In this paper, we present an optimized target-field method for designing a transverse biplanar gradient coil with high linearity, low inductance and small resistance, which can well satisfy the requirements of permanent-magnet MRI systems. In this new method, the current density is expressed by trigonometric basis functions with unknown coefficients in polar coordinates. Following the standard procedures, we construct an objective function with respect to the total square errors of the magnetic field at all target-field points with the penalty items associated with the stored magnetic energy and the dissipated power. By adjusting the two penalty factors and minimizing the objective function, the appropriate coefficients of the current density are determined. Applying the stream function method to the current density, the specific winding patterns on the planes can be obtained. A novel biplanar gradient coil has been designed using this method to operate in a permanent-magnet MRI system. In order to verify the validity of the proposed approach, the gradient magnetic field generated by the resulted current density has been calculated via the Biot–Savart law. The results have demonstrated the effectiveness and advantage of this proposed method.

Keywords: MRI, biplanar gradient coil, optimized target-field method, current density, trigonometric basis function, polar coordinates

(Some figures in this article are in colour only in the electronic version)

1. Introduction

Gradient coils are important parts of magnetic resonance imaging (MRI) systems. They are designed to provide linear magnetic fields along three orthogonal directions over the volume of interest (VOI) with high efficiency. In general, image quality, switching speed and dissipated power of the coil are the three major indices used to evaluate the quality of a gradient coil. The image quality is directly dependent on the linearity of the gradient magnetic field generated by the employed gradient coil. Usually, linearity higher than 95% is required. The switching speed is mainly decided by the inductance of the coil and a high switching speed demands a low inductance. The dissipated power of the coil is highly related to the resistance and a low dissipated power requires

a small resistance. Meanwhile, a small resistance means that the length of the wires on the coil is low and the layout of the wires is simple. Thus, a gradient coil with smaller resistance is easier to manufacture in engineering. For the above reasons, the linearity of the gradient magnetic field, the inductance and the resistance of the coil are the three major factors that should be considered when designing a gradient coil for practical purposes.

Many methods have previously been proposed to design an optimal gradient coil. A widely used method, presented by Turner [1], is called the target-field method. In Turner's original approach, an objective function is constructed to express the gradient magnetic field in terms of the surface current density. Then the desired gradient magnetic field is set over VOI and substituted into the objective function.

Finally by use of the expression of the objective function the surface current density can be obtained and the corresponding winding pattern of the coil can be determined with the aid of a stream function. In Turner's original approach, he only took the linearity of the gradient magnetic field into account during the design. As a result, the inductance of the designed coil is always too large for practical applications. Following Turner's original approach, a number of modified methods were proposed by including the inductance of the coil in the objective function [2–9]. In these methods [2–9], the objective function is written with the gradient magnetic field and the stored magnetic energy (or the inductance), both of which are expressed by the surface current density. Although these minimal-energy methods are theoretically feasible, they are sometimes difficult to implement into practical designs. The main reason is that a large value of power dissipation may be encountered using these methods. This places some challenges on the MRI system. In addition, the winding lines on the surface of the minimal-energy coil are always complex to manufacture [4]. To overcome these problems, Li *et al* [10] proposed a solution for uniplanar gradient coil design in fully open MRI system by further considering the resistance of the coil when building the objective function. In this method [10], the objective function is constructed with respect to the total square errors of the gradient magnetic field at all the desired target-field points with the penalty items associated with the stored magnetic energy and the dissipated power. All three of these items are written with the surface current density. The free space Green function and the Fourier transform component of the current density are used to represent the magnetic field and the stored magnetic energy. In particular, a two-dimensional Fourier series expansion with unknown coefficients in Cartesian coordinates is adopted as the basis functions of the surface current density. In practice, the approach of Li *et al* [10] belongs to the Tikhonov regularization method [11], which has been widely adopted in the design of gradient coils [12–14].

In this paper, based on the work of Li *et al* [10], we present an alternative approach to optimizing the design of transverse biplanar gradient coil for a permanent-magnet MRI system. Instead of using Fourier series expansion with unknown coefficients in Cartesian coordinates as the basis functions of the surface current density, in this approach we employ Morrone's trigonometric basis functions [15] with unknown coefficients in polar coordinates. In order to justify our proposed approach, we utilized the Biot–Savart law to calculate the gradient magnetic field generated by the designed coil.

2. Method

In this paper, the direction of the static main magnetic field (B_0) is along the Z-axis. The Z-gradient coil is the longitudinal gradient coil. The Z-axis component of the magnetic field generated by the Z-gradient coil varies linearly along the Z-axis. The X- and Y-gradient coils are the transverse gradient coils. The Z-axis component of the magnetic field generated by X- or Y-gradient coil varies linearly along the X- or Y-axis.

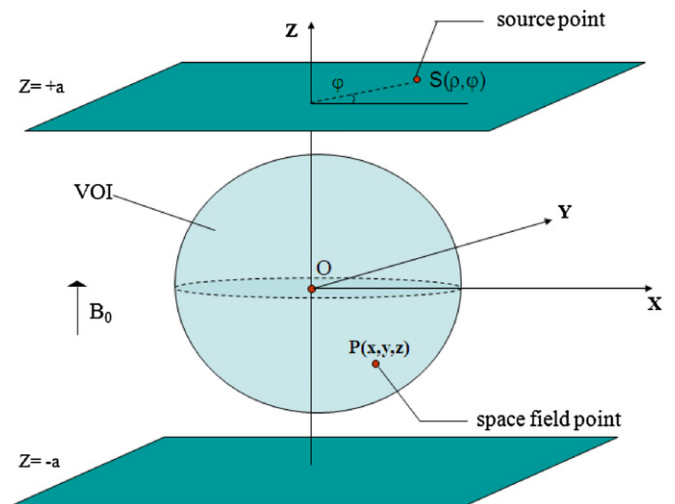


Figure 1. A schematic illustration of the biplanar gradient coil system.

In the rest of this paper, the configuration of the X-gradient coil will be described in detail. The design of the Y-gradient coil follows the same procedure. The schematic diagram of the biplanar X-gradient coil for the permanent-magnet MRI system is shown in figure 1. In this design, the shield coil is not taken into account for the reason that a silicon steel plane used to prevent eddy currents from forming is added in this permanent-magnet MRI system. The top and bottom planes of the gradient coil are located at $Z = +a$ and $Z = -a$. $S(\rho, \varphi)$ denotes a source point on the plane of the gradient coil in polar coordinates while $P(x, y, z)$ represents a space field point in the VOI in Cartesian coordinates.

2.1. Current density basis functions

The current density is distributed on the surface of the two planes at $Z = \pm a$. For transverse gradient coils, the current densities on these two planes are identical.

The radius ρ of each source point meets the following condition: $\rho_0 < \rho < \rho_m$, where ρ_0 is the minimum of the radius and ρ_m is the maximum. The current density vector \vec{J} at any source point must satisfy the continuity equation as follows:

$$\nabla \cdot \vec{J} = 0. \quad (1)$$

The current density at each source point can be expressed by a series of trigonometric basis functions in polar coordinates [15, 16]:

$$\begin{cases} J_\rho(\rho, \varphi) = \sum_{q=1}^Q U_q \frac{1}{\rho} \sin[qc(\rho - \rho_0)] \sin \varphi \\ J_\varphi(\rho, \varphi) = \sum_{q=1}^Q U_q qc \cos[qc(\rho - \rho_0)] \cos \varphi. \end{cases} \quad (2)$$

In (2), $c = \frac{\pi}{\rho_m - \rho_0}$, U_q is the coefficient of the q th current density basis function and is to be determined. Q is the total number of basis functions. In theory, Q trends to infinity. However, in practical calculation, Q is chosen as a finite number which is

accurate enough to approximately establish the current density. It is noted that the expression of the current density meets the continuity equation (1).

2.2. Magnetic field specification

$B_z(x, y, z)$ represents the Z-axis component of the magnetic field at the space field point $P(x, y, z)$. It can be obtained in polar coordinates using the Biot–Savart law with respect to the current density on one plane of the biplanar coil [16]:

$$B_z(x, y, z) = \frac{u_0}{4\pi} \int_{\rho_0}^{\rho_m} \int_0^{2\pi} \frac{\rho \, d\rho \, d\varphi}{R^3} \times [(J_\rho \cos \varphi - J_\varphi \sin \varphi)(y - \rho \sin \varphi) - (J_\rho \sin \varphi + J_\varphi \cos \varphi)(x - \rho \cos \varphi)], \quad (3)$$

where u_0 is the magnetic permeability of vacuum, J_ρ and J_φ are two components of the current density in polar coordinates at the source point on the coil plane, and R is the distance from the source point to the space field point. Since the current densities on the two planes are the same, we can conveniently acquire $B_z(x, y, z)$ generated by the two planes of the coil [16]:

$$B_z(x, y, z) = \frac{u_0}{4\pi} \int_{\rho_0}^{\rho_m} \int_0^{2\pi} \frac{\rho \, d\rho \, d\varphi}{R_+^3} \times [(J_\rho \cos \varphi - J_\varphi \sin \varphi)(y - \rho \sin \varphi) - (J_\rho \sin \varphi + J_\varphi \cos \varphi)(x - \rho \cos \varphi)] + \frac{u_0}{4\pi} \int_{\rho_0}^{\rho_m} \int_0^{2\pi} \frac{\rho \, d\rho \, d\varphi}{R_-^3} [(J_\rho \cos \varphi - J_\varphi \sin \varphi) \times (y - \rho \sin \varphi) - (J_\rho \sin \varphi + J_\varphi \cos \varphi)(x - \rho \cos \varphi)], \quad (4)$$

where $R_\pm = \sqrt{(x - \rho \cos \varphi)^2 + (y - \rho \sin \varphi)^2 + (z \mp a)^2}$, R_+ stands for the distance between the space field point and the source point on the top plane while R_- represents the distance between the space field point and the source point on the bottom plane.

If we substitute the current density with expression (2), B_z then becomes

$$B_z(x, y, z) = \sum_{q=1}^Q U_q M_q(x, y, z), \quad (5)$$

where

$$M_q(x, y, z) = \frac{u_0}{4\pi} \left[\int_{\rho_0}^{\rho_m} \int_0^{2\pi} \frac{d\rho \, d\varphi}{R_+^3} C(\rho, \varphi) + \int_{\rho_0}^{\rho_m} \int_0^{2\pi} \frac{d\rho \, d\varphi}{R_-^3} C(\rho, \varphi) \right], \quad (6)$$

in which

$$C(\rho, \varphi) = (\sin \beta - qc\rho \cos \beta)(y - \rho \sin \varphi) \sin \varphi \cos \varphi - (\sin \beta \sin^2 \varphi + qc\rho \cos \beta \cos^2 \varphi)(x - \rho \cos \varphi) \quad (7)$$

and $\beta = qc(\rho - \rho_0)$. $M_q(x, y, z)$ can be calculated directly, given the location of the space field point in the VOI. For N given points in VOI, we can rewrite expression (5) in matrix form by [16]

$$B_z = M^T U, \quad (8)$$

where

$$B_z = \begin{bmatrix} B_{z1} \\ B_{z2} \\ B_{z3} \\ \vdots \\ B_{zN} \end{bmatrix}, \quad M^T = \begin{bmatrix} M_{11} & M_{12} & M_{13} & \cdots & M_{1Q} \\ M_{21} & M_{22} & M_{23} & \cdots & M_{2Q} \\ M_{31} & M_{32} & M_{33} & \cdots & M_{3Q} \\ \vdots & \vdots & \vdots & \ddots & \vdots \\ M_{N1} & M_{N2} & M_{N1} & \cdots & M_{NQ} \end{bmatrix},$$

$$U = \begin{bmatrix} U_1 \\ U_2 \\ U_3 \\ \vdots \\ U_Q \end{bmatrix}, \quad (9)$$

where B_z represents a column vector of magnetic field values along the Z-axis of all the N space field points. M^T is a matrix which is equal to $N^*Q M_{iq}$. All elements in M^T can be determined according to expression (6). The column vector U denotes the unknown coefficients of current density whose total number is Q .

2.3. Current density solution

In order to optimize the inductance and resistance of the gradient coil, the stored magnetic energy and dissipated power are taken into account in the proposed objective function.

2.3.1. Stored magnetic energy. The stored magnetic energy can be evaluated by the following equation:

$$E = \frac{1}{2} \int_V \vec{A} \cdot \vec{J} \, dv, \quad (10)$$

where \vec{A} is the magnetic potential vector, \vec{J} is the current density vector and V is the distributed volume of the current density. For the biplanar gradient coil system, the above integration is calculated approximately on the planes at $Z = \pm a$. Because of the symmetry between the top and bottom planes, the total stored magnetic energy of the coil is twice that on the top plane. So equation (10) can be written as

$$E = 2E_+ = \iint_S (J_x(x, y)A_x(x, y, a) + J_y(x, y)A_y(x, y, a)) \, dx \, dy, \quad (11)$$

in which

$$\begin{cases} A_x(x, y, a) = \frac{u_0}{4\pi} \iint_S \left(\frac{J_x(x', y')}{R_{a+}} + \frac{J_x(x', y')}{R_{a-}} \right) dx' dy' \\ A_y(x, y, a) = \frac{u_0}{4\pi} \iint_S \left(\frac{J_y(x', y')}{R_{a+}} + \frac{J_y(x', y')}{R_{a-}} \right) dx' dy' \end{cases} \quad (12)$$

and

$$\begin{cases} R_{a+} = \sqrt{(x - x')^2 + (y - y')^2} \\ R_{a-} = \sqrt{(x - x')^2 + (y - y')^2 + 4a^2} \end{cases}, \quad (13)$$

$$\begin{cases} J_x(x, y) = J_{\rho_a} \cos \varphi_a - J_{\varphi_a} \sin \varphi_a \\ J_y(x, y) = J_{\rho_a} \sin \varphi_a + J_{\varphi_a} \cos \varphi_a \\ J_x(x', y') = J_{\rho_b} \cos \varphi_b - J_{\varphi_b} \sin \varphi_b \\ J_y(x', y') = J_{\rho_b} \sin \varphi_b + J_{\varphi_b} \cos \varphi_b. \end{cases} \quad (14)$$

S is the distributed area of the current density on the plane. By employing the expression of the current density (2), the stored magnetic energy in terms of the unknown coefficients can be represented in polar coordinates by

$$E = \frac{1}{2} \sum_{q_a=1}^Q \sum_{q_b=1}^Q U_{q_a} W_{q_a q_b} U_{q_b} = \frac{1}{2} U^T W U, \quad (15)$$

where

$$\begin{aligned} W_{q_a q_b} = & \int_{\rho_0}^{\rho_m} \int_0^{2\pi} (\sin(\beta_a) - q_a c \rho_a \cos(\beta_a)) \sin(\varphi_a) \cos(\varphi_a) \\ & \times \left[\frac{\mu_0}{2\pi} \int_{\rho_0}^{\rho_m} \int_0^{2\pi} \frac{(\sin(\beta_b) - q_b c \rho_b \cos(\beta_b)) \sin(\varphi_b) \cos(\varphi_b)}{R_1} \right. \\ & \times d\rho_b d\varphi_b \\ & + \frac{\mu_0}{2\pi} \int_{\rho_0}^{\rho_m} \int_0^{2\pi} \frac{(\sin(\beta_b) - q_b c \rho_b \cos(\beta_b)) \sin(\varphi_b) \cos(\varphi_b)}{R_2} \\ & \left. \times d\rho_b d\varphi_b \right] d\rho_a d\varphi_a \\ & + \int_{\rho_0}^{\rho_m} \int_0^{2\pi} (\sin(\beta_a) \sin^2(\varphi_a) + q_a c \rho_a \cos(\beta_a) \cos^2(\varphi_a)) \\ & \times \left[\frac{\mu_0}{2\pi} \int_{\rho_0}^{\rho_m} \int_0^{2\pi} \frac{\sin(\beta_b) \sin^2(\varphi_b) + q_b c \rho_b \cos(\beta_b) \cos^2(\varphi_b)}{R_1} \right. \\ & \times d\rho_b d\varphi_b \\ & + \frac{\mu_0}{2\pi} \int_{\rho_0}^{\rho_m} \int_0^{2\pi} \frac{\sin(\beta_b) \sin^2(\varphi_b) + q_b c \rho_b \cos(\beta_b) \cos^2(\varphi_b)}{R_2} \\ & \left. \times d\rho_b d\varphi_b \right] d\rho_a d\varphi_a, \end{aligned} \quad (16)$$

in which

$$\begin{cases} R_1 = \sqrt{(\rho_a \cos \varphi_a - \rho_b \cos \varphi_b)^2 + (\rho_a \sin \varphi_a - \rho_b \sin \varphi_b)^2} \\ R_2 = \sqrt{(\rho_a \cos \varphi_a - \rho_b \cos \varphi_b)^2 + (\rho_a \sin \varphi_a - \rho_b \sin \varphi_b)^2 + 4a^2}, \end{cases} \quad (17)$$

$$\begin{cases} \beta_a = q_a c (\rho_a - \rho_0) \\ \beta_b = q_b c (\rho_b - \rho_0). \end{cases} \quad (18)$$

U denotes the column vector of the unknown coefficients of the current density expression (2) and W represents a squared matrix with the element $W_{q_a q_b}$ determined by equation (16).

2.3.2. Dissipated power. Because of the symmetry between the top and bottom planes, the total dissipated power of the coil is twice that of the top plane. Therefore, the dissipated power on the two planes of the gradient coil can be evaluated by [17]

$$P = 2P_+ = \frac{2\delta}{t} \iint_S ((J_x(x, y))^2 + (J_y(x, y))^2) dx dy, \quad (19)$$

where

$$\begin{cases} J_x(x, y) = J_\rho \cos \varphi - J_\varphi \sin \varphi \\ J_y(x, y) = J_\rho \sin \varphi + J_\varphi \cos \varphi, \end{cases} \quad (20)$$

where δ and t are the resistivity and thickness of the material used in the gradient coil, and S is the distributed area of the current density on the plane.

Similar to the deduction from (11) to (15), the dissipated power in terms of the expression of the current density (2) with

the unknown coefficients can be written in polar coordinates as follows:

$$P = \frac{1}{2} \sum_{q_a=1}^Q \sum_{q_b=1}^Q U_{q_a} G_{q_a q_b} U_{q_b} = \frac{1}{2} U^T G U \quad (21)$$

and

$$\begin{aligned} G_{q_a q_b} = & \frac{4\delta}{t} \int_{\rho_0}^{\rho_m} \int_0^{2\pi} \left\{ \frac{1}{\rho} \sin[q_a c (\rho - \rho_0)] \sin(\varphi) \right. \\ & \times \frac{1}{\rho} \sin[q_b c (\rho - \rho_0)] \sin(\varphi) \\ & + q_a c \cos[q_a c (\rho - \rho_0)] \cos(\varphi) \\ & \left. \times q_b c \cos[q_b c (\rho - \rho_0)] \cos(\varphi) \right\} \rho d\rho d\varphi. \end{aligned} \quad (22)$$

U symbolizes the column vector of the unknown coefficients in current density expression (2) and W represents the matrix with the element $G_{q_a q_b}$ determined by equation (22).

2.3.3. Matrix solution. Solving the coefficients of the current density is a classical problem by constructing an objective function F with respect to the total square errors of the Z-axis component of the magnetic field at all target-field points. Two penalty items associated with the stored magnetic energy and the dissipated power, and weighted by corresponding undetermined penalty factors (λ_1, λ_2), are introduced into the objective function [10, 11]:

$$F = \sum_{j=1}^N (B_{z,j} - B_{zdes,j})^2 + \lambda_1 E + \lambda_2 P, \quad (23)$$

where $B_{z,j}$ represents the Z-axis component of the magnetic field at the (j)th target-field point obtained by expression (5). $B_{zdes,j}$ stands for the Z-axis component of the magnetic field at the (j)th target-field point which is set to meet the specific gradient strength requirement in the VOI.

The objective function can then be rewritten in a simple matrix form as follows:

$$\begin{aligned} F = & (M^T U - B_{zdes})^T (M^T U - B_{zdes}) \\ & + \lambda_1 \frac{1}{2} U^T W U + \lambda_2 \frac{1}{2} U^T G U, \end{aligned} \quad (24)$$

where the j th element of column vector B_{zdes} is $B_{zdes,j}$.

It must be noted that the undetermined penalty factors (λ_1, λ_2) are chosen based on the following criteria: (1) the matrix problem above is well-behaved; (2) the error between the resulting Z-axis component of the magnetic field and the specified Z-axis component of the target magnetic field is within acceptable limits; (3) the stored magnetic energy is low and the dissipated power is appropriate to meet the requirement of the system; (4) the resulting current density distribution is readily implemented into the winding lines on the plane.

In order to minimize F , we must value it at zero with respect to the unknown coefficients of the current density. We can then obtain the optimized current density distribution determined by the estimated U vector. U can be expressed as

$$U = (2MM^T + \lambda_1 W + \lambda_2 G)^{-1} (2M B_{zdes}). \quad (25)$$

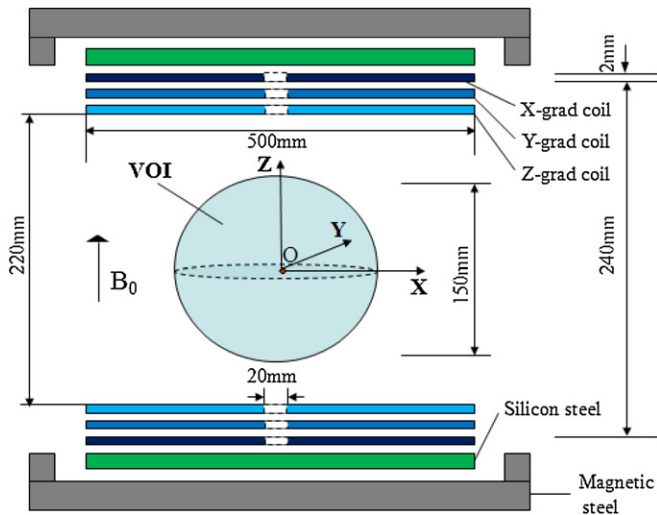


Figure 2. A schematic diagram of a typical permanent-magnet MRI system.

2.4. Stream function

The stream function method [18] is employed to generate the expected winding pattern of the optimized gradient coil. As the current density is required to satisfy the continuity equation (1), the stream function ψ in polar coordinates must satisfy the following terms [16]:

$$\begin{cases} \frac{\partial \psi}{\partial \rho} = -J_\varphi \\ \frac{\partial \psi}{\partial \varphi} = \rho J_\rho. \end{cases} \quad (26)$$

Then we have $\psi(\rho, \varphi) = -\sum_{q=1}^Q U_q \sin[qc(\rho - \rho_0)] \cos \varphi$.

Finally, a series of scattered contours of the stream function are used to produce the current winding pattern on the plane of the coil. If the total number of the expected winding lines on the half-circular plane is set as N_c , then we obtain

$$\psi = \psi_{\min} + (i - 0.5)I \quad i = 1, 2, \dots, N_c \quad (27)$$

in which $I = \frac{(\psi_{\max} - \psi_{\min})}{N_c}$. ψ_{\min} denotes the minimal value of the stream function and ψ_{\max} represents the maximal value on the corresponding half-circular plane. I equals the current on each winding line.

3. Implementation

In this work, a biplanar gradient coil in a typical C-arm permanent-magnet MRI system is illustrated in figure 2. The static main magnetic field B_0 is along the z -direction in Cartesian coordinates and the VOI is a sphere located in the center of the space between the two planes with a diameter of 150 mm. The distance between the two planes of the X-gradient coil is 240 mm and the width of the central space is 220 mm. The thickness of each X-gradient coil plane is 2 mm. The maximum radius of the gradient coil is 250 mm and the minimum radius is 10 mm. In particular, a magnetic steel plane used to generate the static main magnetic field and a silicon steel plane used to prevent eddy currents from forming

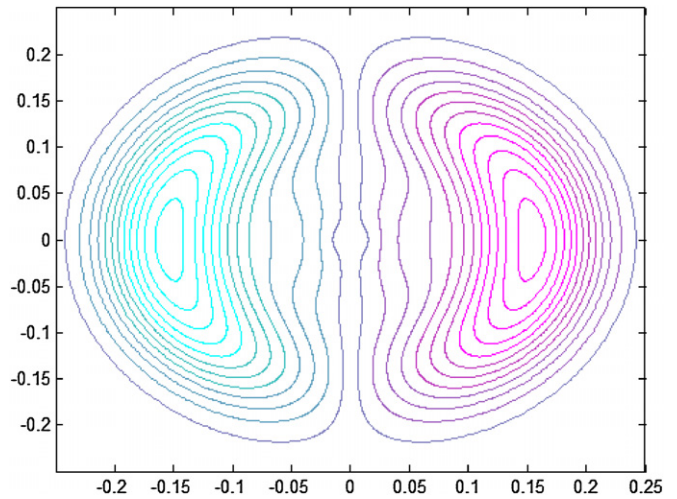


Figure 3. The winding pattern on one plane of the gradient coil.

in the permanent-magnet MRI system are both added to this system.

Because of the symmetry of the biplanar gradient coil system, the magnetic field distribution of all the VOI can be transformed from the first quadrant ($x > 0, y > 0, z > 0$) of the region in Cartesian coordinates. As a result, only the specified target-field points in the first quadrant of the VOI are needed. In this design, we established $N = 48$ target-field points in the first quadrant of VOI. Starting from the original point of the Cartesian coordinate system and along the X -axis, we obtained 12 reference planes perpendicular to the X -axis with a spacing of 6.25 mm between the planes. In each reference plane, on the circle created by intercepting the surface of the VOI sphere with the reference plane, there are four reference points. These points sit at $0^\circ, 30^\circ, 60^\circ$ and 90° with respect to the Y -axis. The Z -axis components of the magnetic field of all the specified target-field points are obtained by equation (28) to generate a gradient strength of 25 mT m^{-1} :

$$B_{zdes,i} = G_x x_i \quad i = 1, 2, \dots, N \quad (28)$$

In (28), $B_{zdes,i}$ represents the specified Z -axis component of the magnetic field at the target-field point whose X coordinate is x_i and $G_x = 25 \text{ mT m}^{-1}$. The resistivity of this coil's material is $1.75 \times 10^{-8} \Omega \text{ m}$ while the material thickness is 2 mm. For practical applications, the inductance is usually set to be smaller than 1 mH and the resistance is in the order of tens of milli-ohms [10]. Finally we set $Q = 4$ in the calculation.

4. Results

By selecting $N_c = 12$, the optimized winding pattern on one plane of the coil was obtained and is given in figure 3.

In order to verify the validity of the proposed approach, we utilized the Biot–Savart law to calculate the gradient magnetic field generated by the resulting current density on the designed coil [16]. Firstly, we set 25 test lines parallel to the X -axis in the first quadrant ($x > 0, y > 0, z > 0$) of VOI in the following steps: (1) we adopted $z_i = (i - 1) \times 15 \text{ mm}$ ($i = 1, 2, 3, 4, 5$) as the corresponding Z coordinate to obtain five test planes

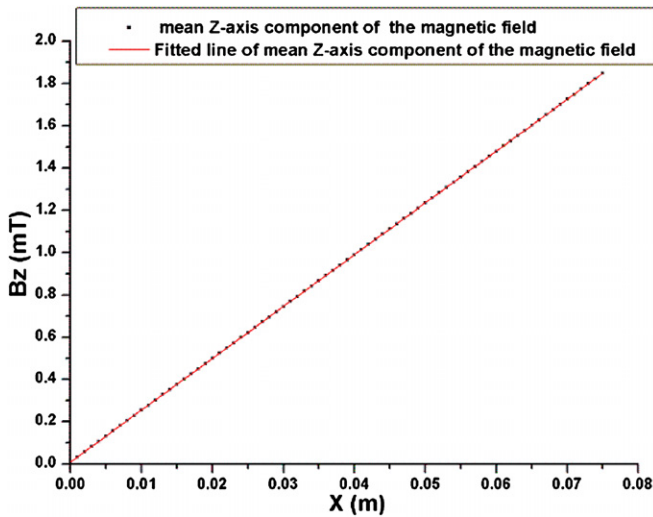


Figure 4. The fitted line of the mean Z-axis component of the magnetic field.

perpendicular to the Z-axis in the first quadrant of VOI; (2) we obtained $y_{ij} = [(j - 1) \times \sqrt{(75^2 - z_i^2)}] / 5$ mm ($j = 1, 2, 3, 4, 5$) on each test plane obtained in step (1) with z_i as the corresponding Z coordinate of each test plane. We took z_i and y_{ij} as the corresponding Z and Y coordinates to altogether obtain 25 test lines parallel to the X-axis. Subsequently, for each of the 25 test lines, we placed the test points 1 mm apart starting from the Y-axis. In this way, we obtained all the test points in the first quadrant ($x > 0, y > 0, z > 0$) of VOI. Then we acquired the mean Z-axis component of the magnetic field on the test points with the same X coordinate and constructed a fitted line based on the mean Z-axis component of the magnetic field and the corresponding X coordinate. The fitted line is shown in figure 4. The mean gradient strength is obtained by the slope of the fitted line.

The nonlinearity of all test points, except the points whose corresponding X coordinates are equal to 0, is represented as follows:

$$\varepsilon = \left| \frac{B_{Z(\text{cal, test-point})} - B_{Z(\text{set, test-point})}}{B_{Z(\text{set, test-point})}} \right| \times 100\%, \quad (29)$$

in which $B_{Z(\text{set, test-point})} = x_{\text{test-point}} \times 25$ mT is the specified Z-axis component of the target magnetic field at the test point and $x_{\text{test-point}}$ is the corresponding X coordinate of the test point. $B_{Z(\text{cal, test-point})}$ is the Z-axis component of the magnetic field at the same test point calculated using the Biot–Savart law.

The results show that the highest nonlinearity of the designed gradient coil at all test points, except those where $x = 0$, is 5.408%; meanwhile, the mean nonlinearity of all test points, except those where $x = 0$, is 0.883%, and the corresponding standard deviation is 0.786%. The mean gradient strength is 24.523 mT m⁻¹ under a current of 8.956 A with 12 winding lines on the half-circular plane, and the efficiency of the coil is 2.738 mT m⁻¹ A⁻¹. The stored magnetic energy and dissipated power of the coil are 0.039 J and 2.454 W, the corresponding inductance is 0.482 mH, and the resistance is 15.298 mΩ on one plane

of the coil. It is clearly demonstrated that the inductance is low and the resistance is small. In addition, it is shown that both the inductance and resistance well satisfy the specific requirements of the permanent-magnet MRI system. It should also be noted that the coil efficiency is high and the pattern of the winding lines of the coil is smooth and acceptable in engineering manufacturing.

Compared with other Tikhonov regularization methods [12–14], the proposed approach can easily guarantee that the designed gradient coil with high linearity, low inductance and small resistance can meet the specific requirements of a permanent-magnet MRI system by adjusting the two penalty factors in the objective function.

5. Conclusion

In this paper, an optimized target-field approach for a transverse biplanar gradient coil is proposed. This method is formulated to optimize the design of gradient coils by taking into account not only the gradient magnetic field at target-field points in VOI, but also the stored magnetic energy and the dissipated power in practical applications. The results indicate that the proposed approach could achieve an optimized transverse gradient coil with high linearity, low inductance and small resistance, which can well meet the requirements of permanent-magnet MRI systems. This new design method can also be applied in the design and optimization of similar planar gradient and shim coils.

Acknowledgments

The authors would like to thank Dr Hua Zhong of Academy for Advanced Interdisciplinary Studies in Peking University for useful discussion and help in English writing. They also want to thank Christopher Calahan for helpful comments on the manuscript.

References

- [1] Turner R 1986 A target field approach to optimal coil design *J. Phys. D: Appl. Phys.* **19** 147–51
- [2] Turner R 1988 Minimum inductance coils *J. Phys. E: Sci. Instrum.* **21** 948–52
- [3] Pissanetzky S 1992 Minimum energy MRI gradient coils of general geometry *Meas. Sci. Technol.* **3** 667–73
- [4] Turner R 1993 Gradient coil design: a review of methods *Magn. Reson. Imaging* **11** 903–20
- [5] Lee S Y, Park B S, Yi J H and Yi W 1997 Planar gradient coil design by scaling the spatial frequencies of minimum-inductance density *Magn. Reson. Med.* **38** 856–61
- [6] Liu H Y and Truwit C L 1998 True energy-minimal and finite-size biplanar gradient coil design for MRI *IEEE Trans. Med. Imaging* **17** 826–80
- [7] Liu H Y 1998 Finite size bi-planar gradient coil for MRI *IEEE Trans. Magn.* **34** 2162–4
- [8] Moon C H, Park H W and Lee S Y 1999 A design method for minimum-inductance planar magnetic-resonance-imaging gradient coils considering the pole-piece effect *Meas. Sci. Technol.* **10** N136–41
- [9] Petropoulos L S 1999 Single gradient coil configuration for MRI systems with orthogonal directed magnetic fields *US Patent 5977771*

- [10] Li X, Xie D X, Wang J M and Zhang X C 2008 Design of finite size uniplanar gradient coil for fully open MRI system with horizontal magnetic field *Int. Conf. on Electromagnetic Field Problems and Applications (Chongqing)* pp 499–502
- [11] Groetsch C W 1984 *The Theory of Tikhonov Regularization for Fredholm Equations of the First Kind* (Boston, MA: Pitman)
- [12] Martens M A, Petropoulos L S, Brown R W, Andrews J H, Morich M A and Patrick J L 1991 Insertable biplanar gradient coils for magnetic resonance imaging *Rev. Sci. Instrum.* **62** 2639–45
- [13] Forbes L K and Crozier S 2004 Novel target-field method for designing shielded biplanar shim and gradient coils *IEEE Trans. Magn.* **40** 1929–38
- [14] Forbes L K, Brideson M A and Crozier S 2005 A target-field method to design circular biplanar coils for asymmetric shim and gradient fields *IEEE Trans. Magn.* **41** 2134–44
- [15] Morrone T 1998 Optimized gradient coils and shim coils for magnetic resonance scanning systems *US Patent* 5760582
- [16] Liu W T, Zu D L, Tang X and Guo H 2007 Target-field method for MRI biplanar gradient coil design *J. Phys. D: Appl. Phys.* **40** 4418–24
- [17] Jin J M 1998 Electromagnetics in magnetic resonance imaging *IEEE Antennas Propag. Mag.* **40** (6) 7–22
- [18] Tomasi D 2001 Stream function optimization for gradient coil design *Magn. Reson. Med.* **45** 505–12